



## Self-induced transparency in InGaAs quantum-dot waveguides

S. Schneider, P. Borri, W. Langbein, U. Woggon, J. Förstner, A. Knorr, R. L. Sellin, D. Ouyang, and D. Bimberg

Citation: *Applied Physics Letters* **83**, 3668 (2003); doi: 10.1063/1.1624492

View online: <http://dx.doi.org/10.1063/1.1624492>

View Table of Contents: <http://scitation.aip.org/content/aip/journal/apl/83/18?ver=pdfcov>

Published by the [AIP Publishing](#)

---



## Re-register for Table of Content Alerts

Create a profile.



Sign up today!



## Self-induced transparency in InGaAs quantum-dot waveguides

S. Schneider, P. Borri,<sup>a)</sup> W. Langbein, and U. Woggon

*Fachbereich Physik, Universität Dortmund, Otto-Hahn Str. 4, D-44227 Dortmund, Germany*

J. Förstner and A. Knorr

*Institut für Theoretische Physik, TU Berlin, Hardenbergstr. 36, D-10623 Berlin, Germany*

R. L. Sellin, D. Ouyang, and D. Bimberg

*Institut für Festkörperphysik, TU Berlin, Hardenbergstr. 36, D-10623 Berlin, Germany*

(Received 15 April 2003; accepted 10 September 2003)

We report the experimental observation and the theoretical modeling of self-induced-transparency signatures such as nonlinear transmission, pulse retardation and reshaping, for subpicosecond pulse propagation in a 2-mm-long InGaAs quantum-dot ridge waveguide in resonance with the excitonic ground-state transition at 10 K. The measurements were obtained by using a cross-correlation frequency-resolved optical gating technique which allows us to retrieve the field amplitude of the propagating pulses. © 2003 American Institute of Physics. [DOI: 10.1063/1.1624492]

Self-induced transparency (SIT) is the nonlinear coherent propagation effect which occurs when optical pulses of duration shorter than the dephasing time and at specific input pulse areas pass through a resonant absorber as if it were transparent. After the first description of this phenomenon by McCall and Hahn,<sup>1</sup> distinguished features of SIT such as nonlinear transmission, pulse retardation, peak amplification, and pulse break-up were observed in a vapor of <sup>87</sup>Rb atoms by Slusher and Gibbs.<sup>2</sup> Because of the many-body Coulomb coupling of the different momentum states in semiconductors, coherent pulse propagation in resonance with excitonic transitions in bulk and quantum-well semiconductors is predicted to be significantly modified compared to the atomic case.<sup>3–6</sup> Excitonic transitions in semiconductors can recover a description in terms of ideal noninteracting two-level systems when considering excitons spatially localized by impurities in bulk semiconductors or three-dimensionally confined excitons in quantum dots (QDs). Indeed nearly lossless pulse propagation in resonance with the donor bound A-exciton state in CdS was measured,<sup>7</sup> and the possibility to observe SIT in self-organized InGaAs QDs has been recently theoretically evaluated.<sup>8</sup> Besides its fundamental interest, SIT has been also exploited for soliton propagation in erbium-doped fibers for optical communication.<sup>9</sup> However, due to the small transition dipole moment ( $\sim 10^{-3}$  D) of the erbium transition, the peak intensity needed for a  $2\pi$  pulse is extremely high in these systems and thus critical with respect to the occurrence of other nonlinear phenomena overlapping with SIT. Using excitonic resonances in semiconductors with large transition dipole moments and long dephasing times, all-optical soliton switches based on SIT for ultrafast applications were modelled.<sup>10</sup> Indeed, excitonic transitions in InGaAs QDs were shown to have transition dipole moments in the range of few tens of debye<sup>11</sup> and dephasing times in the nanosecond range at low temperature,<sup>12</sup> promising for coherent light-matter phenomena with picosecond pulses.

In this work we present the experimental observation and the theoretical modeling of SIT signatures for pulse propagation in the subpicosecond regime in a quantum dot waveguide at low temperature. The investigated sample is a *p-i-n* structure containing three layers of self-organized In<sub>0.7</sub>Ga<sub>0.3</sub>As QDs separated by 35 nm thick GaAs spacers. Two Al<sub>0.7</sub>Ga<sub>0.3</sub>As cladding layers and a ridge structure of 5  $\mu$ m width and 2 mm length provide optical waveguiding. The end facets were tilted to avoid multiple reflections. Details can be found also in Ref. 12. The excitonic ground-state transition shows a Gaussian inhomogeneous broadening of the transitions energies of 60 meV full width at half maximum (FWHM) attributed to fluctuations in the dot size and indium concentration.

A scheme of the experimental setup is shown in Fig. 1. Fourier-limited 0.15 ps laser pulses in resonance with the center of the excitonic ground state transition at 10 K are provided by an optical parametric oscillator (OPO) pumped by a Ti:sapphire laser at 76 MHz repetition rate.

Since short pulse durations result in a sizeable two-photon absorption in the waveguide (see Ref. 11) the pulses are enlarged in time, by shaping their spectrum, to a duration of  $\tau_p = 0.63$  ps (FWHM of the intensity) before being coupled into the transverse electric (TE) polarized waveguide mode using high numerical aperture lenses. The pulses transmitted to the output of the waveguide are cross-correlated with an intense short reference pulse (0.15 ps) of

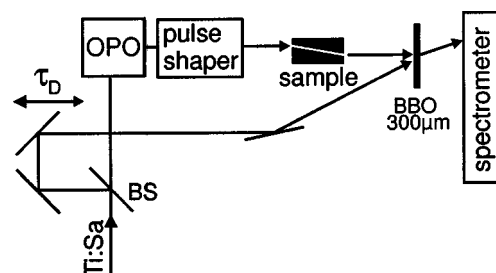


FIG. 1. Scheme of the experimental cross-correlation setup. BS: beam splitter, BBO: beta-bariumborat nonlinear crystal, OPO: optical parametric oscillator.

<sup>a)</sup>Electronic mail: Borri@fred.physik.uni-dortmund.de

relative delay  $\tau_D$  taken from the Ti:sapphire laser. The intensity cross-correlation is obtained by phase-matched sum-frequency generation in a 300  $\mu\text{m}$  thick beta-bariumborate nonlinear crystal. By spectrally resolving the upconverted intensity for different  $\tau_D$  using a spectrometer and a silicon charge coupled device (CCD) camera of 500  $\mu\text{eV}$  resolution (FWHM) we performed a cross-correlation frequency-resolved optical gating (X-FROG, see also Ref. 13). A two-dimensional array of intensities versus optical frequency and delay time  $\tau_D$  is measured, the so-called FROG trace. To retrieve the real-time profile of the field amplitudes of both the transmitted and the reference pulses, a projection algorithm called twin recovery of electric-field envelopes (TREE-FROG)<sup>14</sup> was applied to the trace. This algorithm requires the knowledge of the spectra of both pulses, which were measured using the CCD camera for the reference pulse centered at 740 nm wavelength or a germanium-detector after the spectrometer for the transmitted pulse centered at 1070 nm. Measurements were done for different input pulse areas, by changing the intensity of the input pulse. At very low intensities, because of the insufficient signal-to-noise ratio of the spectrum of the transmitted pulse, we used also another algorithm named X-FROG which requires a full characterized reference pulse alternative to the pulse spectra. In this case the reference pulses retrieved from the TREE-FROG algorithm (which coincided at all intensities) were used for the X-FROG algorithm.

According to the study in Ref. 2 the following important requirements for the observation of the SIT are met in our experiment. The pulse spectral width (3 meV) is much smaller than the inhomogeneous broadening of the ground-state transition. The pulse duration  $\tau_p = 0.63$  ps is much shorter than the dephasing time of the ground-state transition which we measured to be 500 ps at 10 K.<sup>12</sup> The optical density  $\alpha L$  is approximately 5 ( $\alpha$  is the absorption coefficient and  $L$  is the waveguide length).

The intensity cross-correlation versus  $\tau_D$  of the pulse transmitted through the waveguide, obtained by spectrally integrating the FROG trace, is shown in Fig. 2(a) for increasing input pulse area.<sup>15</sup> The corresponding retrieved pulse amplitudes are shown in Fig. 2(b). Side lobes in the field time-profile are present due to the nonperfectly Gaussian spectral filtering in the pulse shaper. We observe two distinct signatures of SIT, namely, pulse retardation and reshaping. However peak amplification and pulse break-up do not occur. In Fig. 2(c) the pulse retardation and reshaping occurring versus pulse area are quantified by the pulse duration (FWHM of the intensity) and the peak position in units of  $\tau_p$ . The ratio of the pulse energy at the output and at the input of the sample, after correcting for coupling and waveguide losses, is also given (dotted line) showing the strong nonlinear absorption bleaching occurring in the region of pulse retardation and reshaping.

In a sample of shorter length, we measured the occurrence of optical Rabi oscillations versus pulse area,<sup>11</sup> a prerequisite of the SIT phenomenon. In that work, we found that the Rabi oscillations were strongly damped versus pulse area and vanished for areas above  $4\pi$ . Comparison with simulations taking into account the spatial distribution of the field in the waveguide mode, the biexcitonic resonance, a finite

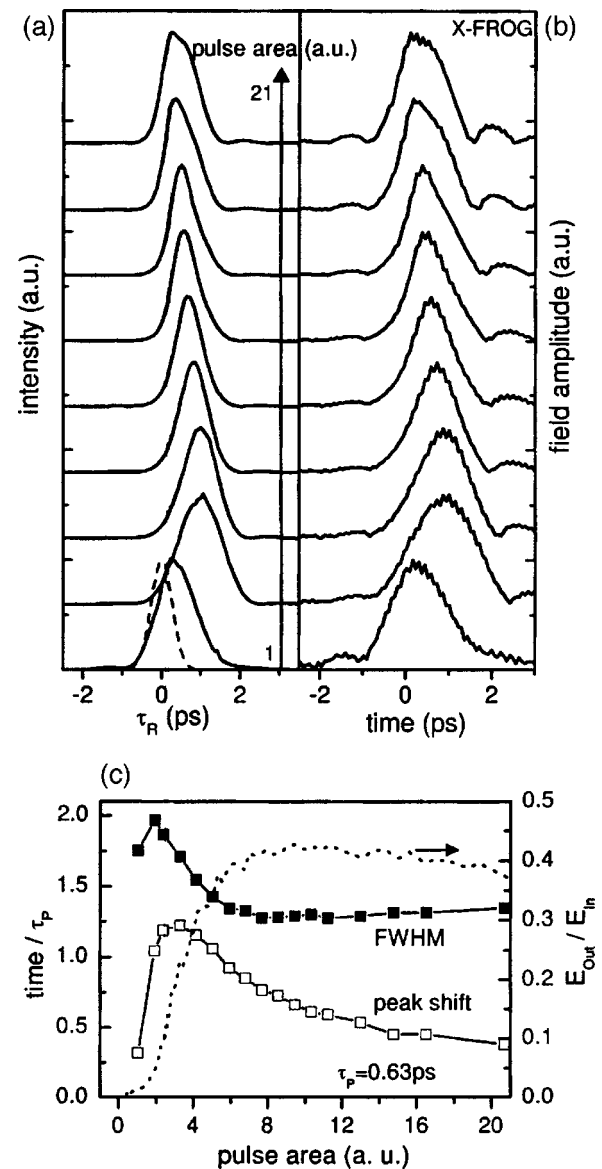


FIG. 2. (a) Intensity cross-correlation of the pulse at the output of the waveguide for increasing pulse area. The output pulse in the linear absorption regime is shown for comparison as dashed line. (b) X-FROG retrieved pulse field amplitudes for the same pulse areas as in (a). Curves in (a) and (b) are normalized to their maximum. (c) Pulse duration (intensity FWHM) and peak position in units of  $\tau_p$  (input pulse duration). The ratio of the pulse energy at the output  $E_{\text{Out}}$  and the input  $E_{\text{In}}$  of the device is also shown versus pulse area (dotted line).

dephasing time, and the inhomogeneous broadening allowed us to conclude that a distribution of the transition dipole moments in the inhomogeneous ensemble was the main cause of the damping versus pulse area of the oscillations. Here, we have extended these simulations including the propagation effects along the waveguide to evaluate the SIT in the structure under investigation. Maxwell's equations were self-consistently evaluated, by applying the slowly varying envelope approximation<sup>16</sup> with restriction to forward propagating modes, together with density matrix equations including excitonic and biexcitonic states (three-level system). Dephasing processes have been approximated by an exponential polarization decay time  $T_2$ .

The calculations were performed considering 3 meV biexciton binding energy, the TE waveguide mode along the

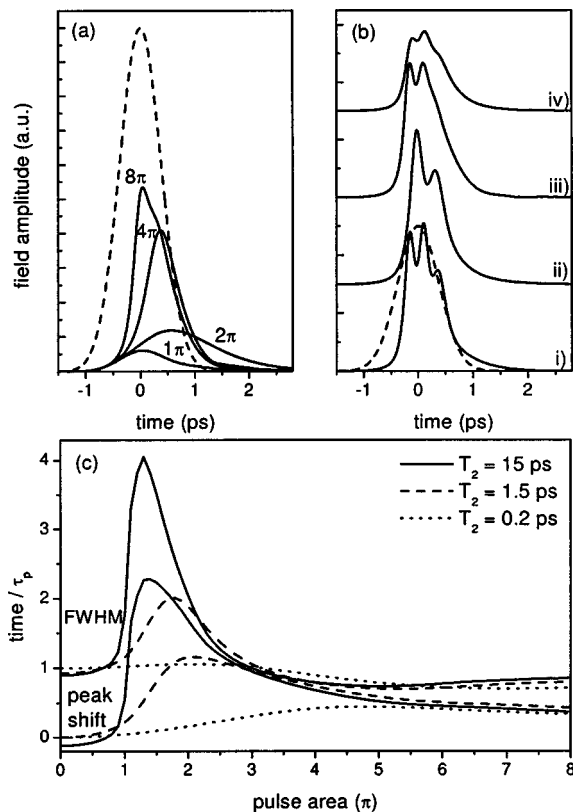


FIG. 3. (a) Calculated field amplitude of pulse after propagation (solid curves) for increasing pulse areas, as indicated. (b)  $8\pi$ -pulse calculated for (i) a two-level system, (ii) a three-level system including the biexciton resonance, (iii) a dipole distribution, and (iv) a nonuniform spatial field profile. The pulse after propagation through a waveguide without dots is shown for comparison as dashed line in (a) and (b). (c) Calculated pulse intensity FWHM and peak position in units of  $\tau_p$  for different dephasing times as indicated.

dot plane as a cosine function, and  $T_2 = 1.5$  ps. The latter value is chosen to take into account that, even if dominated by a 500 ps decay at 10 K, the polarization decay was measured to be strongly nonexponential in Ref. 12 with a fast ( $\sim 1.5$  ps) initial component. Since the inclusion in the calculations of a nonexponential dephasing together with the inhomogeneous broadening is nontrivial, a constant  $T_2 = 1.5$  ps has been chosen here to emphasize the effect of this fast initial polarization decay. Implementations of the theory to include the nonexponential polarization decay are in progress.

Figure 3(a) shows the calculated time-resolved field amplitudes for four different input pulse areas, as indicated. The calculations are in good qualitative agreement with the measured pulse retardation and reshaping. The curves are divided by a factor proportional to the input pulse area for better relative comparison. The dotted line shows the output pulse without the effect of the QD resonant absorber. In order to analyze the effects of the different deviations of the system from the ideal two-level case, we show in Fig. 3(b) the  $8\pi$  pulse after transmission in the case of a two-level system without biexciton, for a plane-wave field profile and without distribution of dipole moments (i), and in the cases where the biexciton resonance (ii), the dipole moment distribution (iii), and the spatial profile of the TE mode (iv) were

separately considered. The comparison shows especially the importance of the spatial averaging in reducing the visibility of peak amplification and pulse break-up. More quantitatively, the agreement between the simulation in Fig. 3(a) and the experiment can be seen in Fig. 3(c), where, for comparison with Fig. 2(c), the calculated peak shift and pulse width are plotted as function of the input pulse area. Calculations were performed for different dephasing times, as indicated, and show that the observed pulse retardation and reshaping indeed rely on a coherent light-matter interaction regime as they are washed out for decreasing  $T_2$  times.

In conclusion, signatures of self-induced transparency have been measured in an InGaAs quantum dot waveguide at low temperature. The experimental results are in good agreement with numerical calculations taking into account realistic parameters intrinsic to a single dot, such as the biexciton resonance and a finite dephasing, as well as ensemble effects, such as an inhomogeneous distribution of dipole moments, and geometrical effects such as the nonuniform spatial profile of the TE mode experienced by the dots along the dot plane in the ridge waveguide under investigation. In particular, the latter effect is found to play a significant role in reducing peak amplification and pulse break-up. This suggests that improved signatures of the SIT phenomenon could be observed in waveguides containing dots only in the central part of the TE mode and opens the work to future developments.

Parts of the work were supported by DFG in the framework Wo477/17-1 and through the Sonderforschungsbereich 296. P.B. is supported by the European Union with the Marie Curie Fellowship HPMF-CT-2000-00843.

<sup>1</sup>S. L. McCall and E. L. Hahn, *Phys. Rev. Lett.* **18**, 908 (1967).

<sup>2</sup>R. E. Slusher and H. M. Gibbs, *Phys. Rev. A* **5**, 1634 (1972).

<sup>3</sup>S. W. Koch, A. Knorr, R. Binder, and M. Lindberg, *Phys. Status Solidi B* **173**, 177 (1992).

<sup>4</sup>H. Giessen, A. Knorr, S. Haas, S. W. Koch, S. Linden, J. Kuhl, M. Hetterich, M. Grün, and C. Klingshirn, *Phys. Rev. Lett.* **81**, 4260 (1998).

<sup>5</sup>A. Schülzgen, R. Binder, M. E. Donovan, M. Lindberg, K. Wundke, H. M. Gibbs, G. Khitrova, and N. Peyghambarian, *Phys. Rev. Lett.* **82**, 2346 (1999).

<sup>6</sup>N. C. Nielsen, S. Linden, J. Kuhl, J. Förstner, A. Knorr, S. W. Koch, and A. Giessen, *Phys. Rev. B* **64**, 245 202 (2001).

<sup>7</sup>M. Jütte, H. Stolz, and W. von der Osten, *J. Opt. Soc. Am. B* **13**, 1205 (1996).

<sup>8</sup>G. Panzarini, U. Hohenester, and E. Molinari, *Phys. Rev. B* **65**, 165 322 (2002).

<sup>9</sup>M. Nakazawa, Y. Kimura, K. Kurokawa, and K. Suzuki, *Phys. Rev. A* **45**, R23 (1992).

<sup>10</sup>A. Guzman, M. Romagnoli, and S. Wabnitz, *Appl. Phys. Lett.* **56**, 614 (1990).

<sup>11</sup>P. Borri, W. Langbein, S. Schneider, U. Woggon, R. L. Sellin, D. Ouyang, and D. Bimberg, *Phys. Rev. B* **66**, 081 306(R) (2002).

<sup>12</sup>P. Borri, W. Langbein, S. Schneider, U. Woggon, R. L. Sellin, D. Ouyang, and D. Bimberg, *Phys. Rev. Lett.* **87**, 157 401 (2001).

<sup>13</sup>S. Linden, H. Giessen, and J. Kuhl, *Phys. Status Solidi B* **206**, 119 (1998).

<sup>14</sup>K. W. DeLong, R. Trebino, and W. E. White, *J. Opt. Soc. Am. B* **12**, 2463 (1995).

<sup>15</sup>The estimate of the pulse area in radians requires the knowledge of the waveguide-mode size, of the transition dipole moment, of the pulse energy coupled into the waveguide and can be quite inaccurate. Using the parameters in Ref. 11, the values shown in Fig. 2 are in units of  $\pi$ .

<sup>16</sup>L. Allen and J. H. Eberly, *Optical Resonance and Two Level Atoms* (Wiley, Chichester, England, 1975).